Greek Letters

α = volumetric gas content of liquid slug, vol. gas/vol. pipe
Δ = denotes a difference
$\Delta\rho$ = density difference between the liquids
ρ, ρ_L = liquid density
ρ_c = density of the continuous phase
ρ_G = gas density
τ_w = wall shear acting on liquid slugs
μ = liquid viscosity
μ_G = gas viscosity

Subscripts

i = specific gas bubble in macroscopic model (Figure 1)
D = dimensionless quantity
G = gas phase
L = liquid phase
N = number of gas bubbles in macroscopic model

Superscripts

f = liquid film around gas bubble
$\overline{\ }$ = time-averaged quantity

LITERATURE CITED

1. Balzhiser, R. E., et al., *ASD Tech. Rept. 61-594*, Univ. of Michigan, Ann Arbor, Michigan (December, 1961).
2. Bennett, J. A. R., United Kingdom Atomic Energy Authority, *A.E.R.E. CE/R 2497* (March, 1958).
3. Gresham, W. A., P. A. Foster, and R. J. Kyle, *W.A.D.C. Tech. Rept. 55-422*, Georgia Institute of Technology, Atlanta, Georgia (June, 1955).
4. Isbin, H. S., R. H. Moen, and D. R. Mosher, United States Atomic Energy Commission, *A.E.C.U. -2994* (November, 1954).
5. Dumitrescu, D. T., *Z. Angew. Math. Mech.*, **23**, 139 (1943).
6. Davies, R. M., and G. I. Taylor, *Proc. Roy. Soc.*, **200A**, 375 (1950).
7. Griffith, P., and G. B. Wallis, *Trans. Am. Soc. Mech. Engrs.*, **83C**, 307 (1961).
8. Laird, A. E. K., and D. Chisholm, *Ind. Eng. Chem.*, **48**, 1361 (1956).
9. Nicklin, D. J., J. O. Wilkes, and J. F. Davidson, *Trans. Inst. Chem. Engrs.*, **40**, 61 (1962).
10. Moissis, R., and P. Griffith, *Trans. Am. Soc. Mech. Engrs.*, **84C**, 29 (1962).
11. Street, J. R., and M. R. Tek, *A.I.Ch.E. J.*, **11**, No. 4 (1965).
12. Street, J. P., Ph.D. thesis, Univ. of Michigan, Ann Arbor, Michigan (September, 1962).
13. Kadlec, R. H., Ph.D. thesis, Univ. of Michigan, Ann Arbor, Michigan (September, 1961).
14. Harmathy, T. Z., *A.I.Ch.E. Journal*, **6**, 281 (1960).

Manuscript received May 15, 1964; revision received November 18, 1964; paper accepted January 22, 1965. Paper presented at A.I.Ch.E. San Juan meeting.

Unsteady Heat Transfer to Slug Flows: Effect of Axial Conduction

S. C. CHU and S. G. BANKOFF

Northwestern University, Evanston, Illinois

Solutions are obtained for three illustrative cases of unsteady heat transfer to slug flows, taking axial conduction into account. The magnitude of the correction to the solutions neglecting this effect is shown to be quite appreciable near the leading edge. In agreement with previous steady state estimates, the axial conduction correction becomes negligible for Peclet numbers in excess of 100.

Slug flows comprise the class of incompressible flows in which the velocity field is everywhere uniform. Despite their relative simplicity, solutions of the equations for unsteady transport of heat or mass to slug flows have not been extensively investigated, possibly because there are at least three independent variables. Such problems arise in such diverse applications as the continuous annealing of bars and the heating of oil or gas in underground strata. For definiteness it will be assumed herein that the diffusant is heat; the authors shall also be concerned only with problems in which two space variables, as well as time, are involved, and in which the fluid velocity remains constant with time. Such problems are conveniently solved by multiple transform methods, with the Laplace transform to remove the time variable, and a finite Sturm-Liouville transform or Laplace transform to remove one of the space variables. In some cases it is permissible to neglect axial conduction, and for the interested reader, a number of problems of this type are solved in reference *1*. Siegel (*2*) has shown that these problems can also be solved by considering separately the fluid particles which were before and beyond the tube leading edge at the instant of imposition of the new boundary conditions. No heat exchange can occur between these two regions on account of the neglect of axial conduction. Hence, it is possible to solve for the temperature in each region sep-

S. C. Chu is with Allied Chemical and Dye Corporation, Hopewell, Virginia.

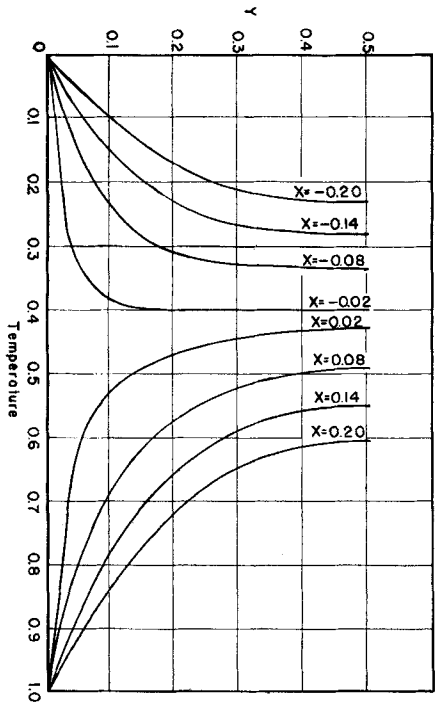

Fig. 1. Steady state temperature profiles at several axial positions ($N_{Pe} = 1$) for infinite parallel plates with axial conduction.

arately, with a consequent reduction in the number of independent variables in each region. The same results can be obtained by multiple transform methods with approximately the same labor, and without recourse to physical arguments.

When axial conduction can no longer be neglected, however, the power of the transform method becomes evident. In this paper three illustrative problems are solved, and numerical correction terms for the effect of axial conduction obtained. In the first two problems the fluid entering the parallel plate or round conduit is at a specified temperature, which is an appropriate boundary condition when a well-stirred reservoir precedes the conduit. Such a condition is frequently appropriate for thermal injection in porous media. The third problem involves a moving infinite slab upon whose surface a step change in temperature is suddenly imposed for $x > 0$. Such problems arise, for example, in continuous heat treatment processes.

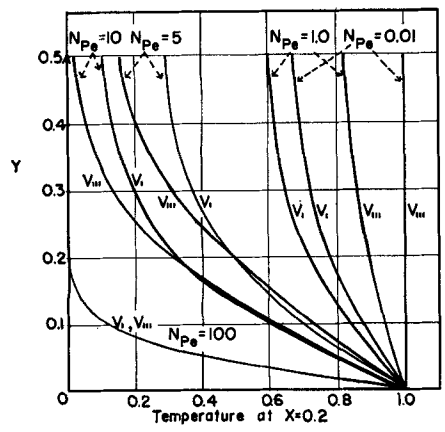

Fig. 2. Steady state temperature profiles for various Peclet numbers at $X = 0.2$, with (*I*) and without (*III*) axial conduction.

No previous studies of the effect of axial conduction on unsteady transfer to slug flows has come to the authors' attention, but the analogous steady state problems have been investigated by Schneider (3), who found these effects to be important only for Peclet numbers less than 100. Extensions to Poiseuille flows were made by Bodnarescu (4), Singh (5, 6), Labuntsov (7), Agrawal (8), and Pahor and Strand (9). Horvay (10) and Horvay and DaCosta (11) extended the solutions for moving slabs and tubes by considering mixed boundary conditions, using the Wiener-Hopf technique.

SEMI-INFINITE TUBE

When one assumes constant thermal properties of fluid and uniform velocity in the tube, the equation describing the system is

$$\frac{\partial v}{\partial t} + U\frac{\partial v}{\partial x} = \kappa\left[\frac{\partial^2 v}{\partial x^2} + \frac{1}{r}\frac{\partial}{\partial r}\left(r\frac{\partial v}{\partial r}\right)\right],$$

$$v = v(t, x, r); \quad t > 0, \quad x > 0, \quad 0 \leq r \leq b \qquad (1)$$

with initial condition $v(0, x, r) = 0$, and boundary conditions $v(t, 0, r) = v_o$, $v(t, x, b) = v_w$, $v(t, \infty, r)$ and $v(t, x, 0)$ finite. In dimensionless form the equation becomes

$$\frac{\partial V}{\partial \tau} + B\frac{\partial V}{\partial X} = \frac{\partial^2 V}{\partial X^2} + \frac{1}{R}\frac{\partial}{\partial R}\left(R\frac{\partial V}{\partial R}\right),$$

$$V = V(\tau, X, R); \quad \tau > 0, \quad X > 0, \quad 0 \leq R \leq 1 \qquad (2)$$

with initial condition $V(0, X, R) = 0$, and boundary conditions $V(\tau, 0, R) = 0$, $V(\tau, X, 1) = 1$, $V(\tau, \infty, R)$ and $V(\tau, X, 0)$ finite.

The problem will be solved by the successive application of the Laplace transform with respect to the time variable

$$V_p = \int_o^\infty V e^{-p\tau}\, d\tau$$

and a Hankel transform with respect to the radial coordinate

$$V_H = \int_o^1 VR J_o(\xi_i R)\, dR$$

where, in view of the boundary condition at $R = 1$, the Bessel function eigenvalues are given by $J_o(\xi_i) = 0$, $i = 1, 2, \ldots$.

Applying the Hankel transform operator to Equation (2), one obtains (10)

$$\frac{\partial V_H}{\partial \tau} + B\frac{\partial V_H}{\partial X} = \frac{\partial^2 V_H}{\partial X^2} - A - \xi_i^2 V_H \qquad (3)$$

where $A = \xi_i J_o'(\xi_i)$, subject to the initial condition $V_H(0, X, \xi) = 0$ and the boundary conditions $V_H(\tau, \infty, \xi)$ finite; $V_H(\tau, 0, \xi) = 0$. Upon operating with the Laplace transform, Equation (3) becomes

Table 1. Temperature Near the Wall at $X = 0$ for Infinite Parallel Plate Case, Taking Into Account Axial Conduction, Equation (28)

Y \ τ	10^{-5}	10^{-4}	10^{-3}	10^{-2}	10^{-1}	4×10^{-1}
10^{-5}	0.4993	0.4997	0.4999	0.5000	0.5000	0.5000
10^{-4}	0.4925	0.4971	0.4991	0.4997	0.4999	0.4999
10^{-3}	0.4253	0.4972	0.4907	0.4966	0.4985	0.4995
10^{-2}	0.0000	0.2388	0.4087	0.4674	0.4861	0.4992
10^{-1}	0.0000	0.0000	0.0124	0.2314	0.3995	0.4932

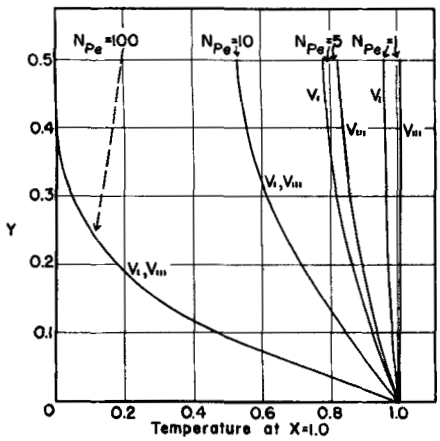

Fig. 3. Steady state temperature profiles for various Peclet numbers at X = 1.0, with (I) and without (III) axial conduction.

$$\frac{d^2V_{Hp}}{dX^2} - B\frac{dV_{Hp}}{dX} - (\xi_i^2 + p)V_{Hp} = \frac{A}{p} \tag{4}$$

subject to the two-point boundary conditions $V_{Hp}(p, 0, \xi) = 0$; $V_{Hp}(p, \infty, \xi)$ finite. The solution of this linear inhomogeneous differential equation is

$$V_{Hp} = \frac{A}{p(p+\xi_i^2)}\{-1 + \exp[(a_2 - \sqrt{a_3^2 + p})\,X]\} \tag{5}$$

where $a_2 = \dfrac{B}{2}$ and $a_3 = \sqrt{\xi_i^2 + \dfrac{B^2}{4}}$

The evaluation of the inverse Laplace transform is not difficult, and leads to

$$V_H = -\frac{A}{\xi_i^2}\left\{1 - e^{-\xi_i^2\tau} + \frac{e^{a_2X}}{2}\left[e^{a_2X-\xi_i^2\tau}\,\mathrm{erfc}\left(\frac{X}{2\sqrt{\tau}} + a_2\sqrt{\tau}\right) + e^{-a_2X-\xi_i^2\tau}\,\mathrm{erfc}\left(\frac{X}{2\sqrt{\tau}} - a_2\sqrt{\tau}\right) - e^{a_3X}\,\mathrm{erfc}\left(\frac{X}{2\sqrt{\tau}} + a_3\sqrt{\tau}\right) - e^{-a_3X}\,\mathrm{erfc}\left(\frac{X}{2\sqrt{\tau}} - a_3\sqrt{\tau}\right)\right]\right\} \tag{6}$$

$$\equiv -\frac{A}{\xi_i^2}\,g_i(X, \tau)$$

The Hankel transform inversion (*10*) then gives

$$V = -2\sum_{i=1}^{\infty}\frac{J_o(R\xi_i)\;g_i(X,\tau)}{\xi\,J_o'(\xi_i)} \tag{7}$$

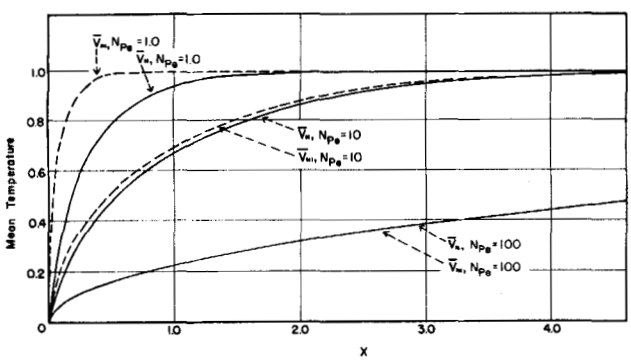

Fig. 4. Steady state mean temperature with (II) and without (III) axial conduction for various Peclet numbers.

As τ becomes large, the temperature approaches its steady state distribution:

$$V = -2\sum_{i=1}^{\infty}\frac{J_o(R\xi_i)}{\xi\,J_o'(\xi_i)}\{1 - e^{-a_3X+a_2X}\} \tag{8}$$

The mean temperature may be expressed as

$$\bar{V} = \frac{\int_o^1 r\,V\,dr}{\int_o^1 r\,dr} = 4\sum_{i=1}^{\infty}\frac{1}{\xi_i^2}\,g_i(X,\tau) \tag{9}$$

and the local Nusselt number as

$$N_{Nu} = \frac{(\partial V/\partial R)_{R=1}}{1-\bar{V}} = \frac{-2}{1-\bar{V}}\sum_{i=1}^{\infty}g_i(X,\tau) \tag{10}$$

SEMI-INFINITE PARALLEL PLATES

When one again assumes constant physical properties and slug flow, the equation describing the system is

$$\frac{\partial v}{\partial t} + U\frac{\partial v}{\partial x} = \kappa\left(\frac{\partial^2 v}{\partial y^2} + \frac{\partial^2 v}{\partial x^2}\right),$$

$$v = v(t, x, y), \quad t > 0, \quad x > 0, \quad 0 \le y \le b \tag{11}$$

subject to the initial condition $v(0, x, y) = v_o$, and the boundary conditions $v(t, 0, y) = v_o$, $v(t, x, 0) = v_w$, $v(t, x, b) = v_w$, and $v(t, \infty, y)$ finite.

In dimensionless form the system becomes

$$\frac{\partial V}{\partial \tau} + B\frac{\partial V}{\partial X} = \frac{\partial^2 V}{\partial X^2} + \frac{\partial^2 V}{\partial Y^2} \tag{12}$$

with I.C. $V(0, X, Y) = 0$; B.C. $V(\tau, 0, Y) = 0$, $V(\tau, X, 0) = 1$, $V(\tau, X, 1) = 1$, and $V(\tau, \infty, Y)$ finite.

When one introduces now the Fourier sine transform

$$V_s = \int_o^1 V \sin n\pi Y\,dY \tag{13}$$

followed again by the Laplace transform, Equation (12) becomes

$$pV_{sp} + B\frac{dV_{sp}}{dx} = \frac{n\pi}{p}[1 + (-1)^{n+1}] - (n\pi)^2 V_{sp} + \frac{d^2V_{sp}}{dX^2} \tag{14}$$

subject to the two-point boundary conditions $V_{sp}(p, \infty, n)$ finite, and $V_{sp}(p, 0, n) = 0$. Upon rearranging Equation (14) one readily finds the solution to be

$$V_{sp} = \frac{n\pi[1 + (-1)^{n+1}]}{p(p + n^2\pi^2)}\left\{1 - \exp\left(\frac{XB}{2} - \frac{X}{2}\sqrt{B^2 + 4p + 4n^2\pi^2}\right)\right\} \tag{15}$$

The Laplace transform inversion is performed by standard manipulations:

$$V_s = \frac{D}{(n\pi)^2}\left\{1 - e^{(n\pi)^2\tau} + \frac{e^{a_2X}}{2}\left[e^{a_2X-(n\pi)^2\tau}\,\mathrm{erfc}\left(\frac{X}{2\sqrt{\tau}} + a_2\sqrt{\tau}\right) +\right.\right.$$

$$e^{-a_2X-(n\pi)^2\tau}\operatorname{erfc}\left(\frac{X}{2\sqrt{\tau}}-a_2\sqrt{\tau}\right)-$$

$$e^{a_1X}\operatorname{erfc}\left(\frac{X}{2\sqrt{\tau}}+a_1\sqrt{\tau}\right)-e^{-a_1X}\operatorname{erfc}\left(\frac{X}{2\sqrt{\tau}}-a_1\sqrt{\tau}\right)\Bigg] \tag{16}$$

$$\equiv\frac{D}{(n\pi)^2}\left[1-h_n(X,\tau)\right]$$

where $a_1^2=\frac{B^2}{4}+(n\pi)^2$, $D=n\pi[1+(-1)^{n+1}]$, and $a_2=\frac{B}{2}$. The Fourier sine inversion series gives

$$V=2\sum_{n=1}^{\infty}\frac{[1+(-1)^{n+1}]\sin n\pi Y}{n\pi}\left[1-h_n(X,\tau)\right] \tag{17}$$

As $\tau\to\infty$, the steady state temperature profile is approached:

$$V=2\sum_{n=1}^{\infty}\frac{[1+(-1)^{n+1}]}{n\pi}\sin n\pi Y\,(1-e^{-a_1X+a_2X}) \tag{18}$$

The mean temperature is now

$$\overline{V}=\int_0^1 V\,dY=1-8\sum_{n=1,3,5\ldots}^{\infty}\left(\frac{1}{n\pi}\right)^2 h_n(X,\tau) \tag{19}$$

and the Nusselt number is

$$N_{Nu}=\frac{(\partial V/\partial Y)_{Y=1}}{1-\overline{V}}=\frac{4}{1-\overline{V}}\sum_{n=1,3,5\ldots}^{\infty}h_n(X,\tau) \tag{20}$$

INFINITE PARALLEL PLATES

The system differs from the previous one in that the axial variable X now extends over the interval $(-\infty,\infty)$. Again, the fluid is initially everywhere at a uniform temperature, and at time $t=0$ a step change in wall temperature is imposed for $X>0$. The dimensionless governing equation is then

$$\frac{\partial V}{\partial\tau}+B\frac{\partial V}{\partial X}=\frac{\partial^2V}{\partial X^2}+\frac{\partial^2V}{\partial Y^2} \tag{21}$$

subject to the initial condition $V(0,X,Y)=0$, and boundary conditions $V(\tau,X,0)=V(\tau,X,1)=H(X)$ [where $H(X)$ is the unit step function], while $V(\tau,\infty,Y)$ and $V(\tau,-\infty,Y)$ remain finite.

Again applying successively the finite Fourier sine transform and the Laplace transform, one gets

$$\frac{d^2V_{sp}}{dX^2}-B\frac{dV_{sp}}{dX}-A_1V_{sp}=-\frac{D}{p}H(X) \tag{22}$$

where $A_1=p+(n\pi)^2$. This is an ordinary nonhomogeneous differential equation whose solution is of the form

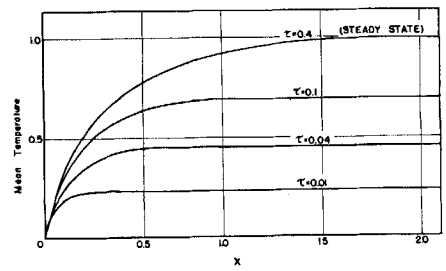

Fig. 5. Unsteady local mean temperature vs. X ($N_{Pe}=1$) for semi-infinite parallel plates with axial fluid conduction.

$$V_{sp}=c_1H(-X)e^{\frac{X}{2}(B+\sqrt{B^2+4A})}+c_2e^{\frac{X}{2}(B-\sqrt{B^2+4A})}+\frac{D}{Ap}H(X) \tag{23}$$

when one takes into account that the temperature is everywhere finite.

From continuity of temperature and heat flux at $X=0$, one finds

$$c_1=c_2+\frac{D}{Ap}, \tag{24}$$

$$c_2(B-\sqrt{B^2+4A})=c_1(B+\sqrt{B^2+4A}) \tag{25}$$

The constants can be thus determined, giving

$$V_{sp}=-\frac{D}{2Ap}\left\{\left\{\frac{B+\sqrt{B^2+4A}}{\sqrt{B^2+4A}}e^{\frac{X}{2}(B-\sqrt{B^2+4A})}-2\right\}H(X)+\frac{B-\sqrt{B^2+4A}}{\sqrt{B^2+4A}}H(-X)e^{\frac{X}{2}(B+\sqrt{B^2+4A})}\right\} \tag{26}$$

After double inverse transformation [for details see (*1*)], the unsteady temperature distribution is obtained as a function of time and position:

For $X\leq 0$

$$V=\sum_{n=1}^{\infty}D\,e^{a_2X}\sin n\pi Y\left\{\frac{1}{2a_1(a_1+a_2)}e^{a_1X}\operatorname{erfc}\left[\frac{-X}{2\sqrt{\tau}}-a_1\sqrt{\tau}\right]+\frac{1}{2a_1(a_1-a_2)}e^{-a_1X}\operatorname{erfc}\left[-\frac{X}{2\sqrt{\tau}}+a_1\sqrt{\tau}\right]+\frac{1}{a_2^2-a_1^2}e^{-a_2X+(a_2^2-a_1^2)\tau}\operatorname{erfc}\left[-\frac{X}{2\sqrt{\tau}}+a_1\sqrt{\tau}\right]\right\} \tag{27}$$

and for $X\geq 0$

$$V=2\sum_{n=1}^{\infty}D\sin n\pi Y\left\{\frac{1}{(n\pi)^2}\left[1-e^{-(n\pi)^2\tau}\right]-\frac{e^{a_2X}}{2}\left[\frac{e^{-a_1X}}{2a_1(a_1-a_2)}\operatorname{erfc}\left(\frac{X}{2\sqrt{\tau}}-a_1\sqrt{\tau}\right)+\frac{e^{a_1X}}{2a_1(a_1+a_2)}\operatorname{erfc}\left(\frac{X}{2\sqrt{\tau}}+a_1\sqrt{\tau}\right)+\frac{e^{-a_2X+(a_2^2-a_1^2)\tau}}{a_2^2-a_1^2}\operatorname{erfc}\left(\frac{X}{2\sqrt{\tau}}-a_2\sqrt{\tau}\right)\right]\right\} \tag{28}$$

These equations are readily manipulated to give the local cross-sectional mean temperature, the local Nusselt number, and the steady state temperature profile (*1*). It is of interest that the steady state solutions obtained by Schneider (*3*) and Wilson (*13*) by separation-of-variable methods are identical with the ones obtained here as limiting cases of the transient solutions:

$$V = \sum_{n=1}^{\infty} D\, e^{a_2 X} \sin n\pi Y \left\{ \frac{e^{a_1 X}}{a_1(a_1 + a_2)} \right\}, \quad \text{for } X < 0 \qquad (29)$$

and

$$V = 2\sum_{n=1}^{\infty} D \sin n\pi Y \left\{ \frac{1}{(n\pi)^2} - \frac{e^{a_2 X - a_1 X}}{2a_1(a_1 - a_2)} \right\} \quad \text{for } X > 0 \qquad (30)$$

NUMERICAL RESULTS

Of particular concern here is the error associated with the neglect of axial conduction. The solutions given in (*1*) for the local fluid temperature, the mean fluid temperature at any downstream location, and the local Nusselt number may be written as follows:

$$V_{III} = 2\sum_{n=1}^{\infty} \frac{D \sin n\pi Y}{(n\pi)^2} \left\{ 1 - e^{-(n\pi)^2 \tau} \left[1 - H\left(\tau - \frac{X}{B}\right) \right] - e^{-(n\pi)^2 \frac{X}{B}} H\left(\tau - \frac{X}{B}\right) \right\} \qquad (31)$$

$$\overline{V}_{III} = 8\sum_{n=1,3,5,\ldots}^{\infty} \frac{1}{(n\pi)^2} \left\{ 1 - e^{-(n\pi)^2 \tau} \left[1 - H\left(\tau - \frac{X}{B}\right) \right] - e^{-(n\pi)^2 \frac{X}{B}} H\left(\tau - \frac{X}{B}\right) \right\} \qquad (32)$$

$$Nu_{III} = \frac{\sum_{n=\text{odd}}^{\infty} \left\{ e^{-(n\pi)^2 \tau} \left[1 - H\left(\tau - \frac{X}{B}\right) \right] + e^{-(n\pi)^2 \frac{X}{B}} H\left(\tau - \frac{X}{B}\right) \right\}}{2\sum_{n=\text{odd}}^{\infty} \frac{1}{(n\pi)^2} \left\{ e^{-(n\pi)^2 \tau} \left[1 - H\left(\tau - \frac{X}{B}\right) \right] + e^{-(n\pi)^2 \frac{X}{B}} H\left(\tau - \frac{X}{B}\right) \right\}} \qquad (33)$$

The subscript *III* stands for the semi-infinite parallel plate geometry, neglecting axial conduction. For the solutions for the infinite and semi-infinite plate geometries, taking into account axial conduction, the authors employ the subscripts *I* and *II*, respectively. Both steady state and transient results were obtained. The computations were performed on an IBM-709 computer, and since an infinite series of error functions are involved, the accuracy of the error function subroutine was checked to eight decimal places.

STEADY STATE

Typical dimensionless temperatures in the neighborhood of the origin for $I(N_{Pe} = 1)$ are shown in Figure 1. The asymmetry is due to the convection effect, modified by axial conduction, and increases as the Peclet number is increased. In Table 1 some temperatures close to the wall at $X = 0$ are presented. A limiting temperature of 0.5 is observed at the wall, to be expected from the properties of orthogonal expansions at a point of finite discontinuity. In Figures 2 and 3, the *I* and *III* temperature profiles at two downstream locations are plotted with Peclet number as the parameter. At lower Peclet numbers the axial conduction correction is appreciable but becomes negligible for $N_{Pe} > 100$ at $X = 0.2$ and for $N_{Pe} > 10$ at $X = 1.0$, illustrating that axial conduction effects are accentuated in the neighborhood of the leading edge. The temperature difference undergoes an interesting change in sign across the cross section at $X = 0.2$ for $N_{Pe} = 5$ and 10. This is attributed to the axial conduction effect dominating near the wall, whereas convection dominates some distance away from the wall. However, for $N_{Pe} = 100$, the axial conduction effect is everywhere small, and the difference becomes very small.

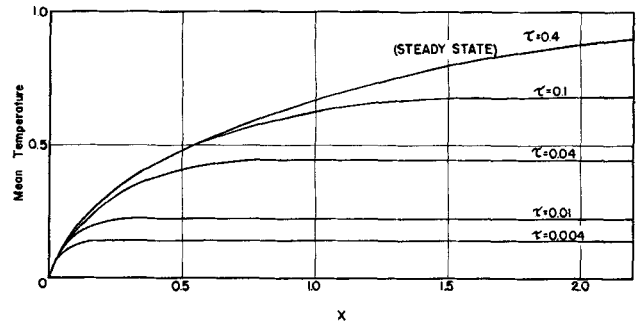

Fig. 6. Unsteady local mean temperature vs. X ($N_{Pe} = 10$) for semi-infinite parallel plates with axial fluid conduction.

The cross-sectional local mean temperature for cases *II* and *III* were calculated from Equations (19) and (32) and are plotted in Figure 4. One sees again that there is a considerable axial conduction effect at $N_{Pe} = 1.0$, which diminishes rapidly as the Peclet number increases.

UNSTEADY STATE

A series of mean temperature profiles for case *II* are plotted for various times during the transient in Figures 5 and 6 for $N_{Pe} = 1.0$ and 10, respectively. The curves all pass through the origin, reflecting the boundary condition at $X = 0$ for the semi-infinite plate geometry. The mean temperature approaches an asymptotic value at large downstream distances, corresponding to the pure conduc-

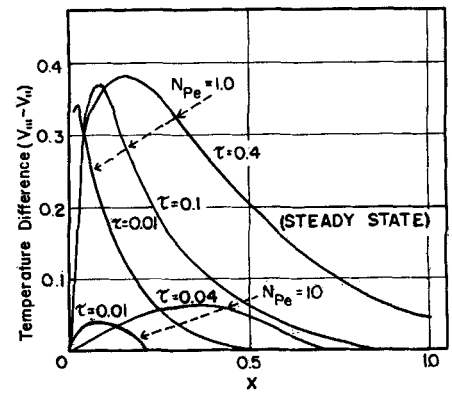

Fig. 7. Mean temperature difference between solutions with and without axial fluid conduction for various times and Peclet numbers.

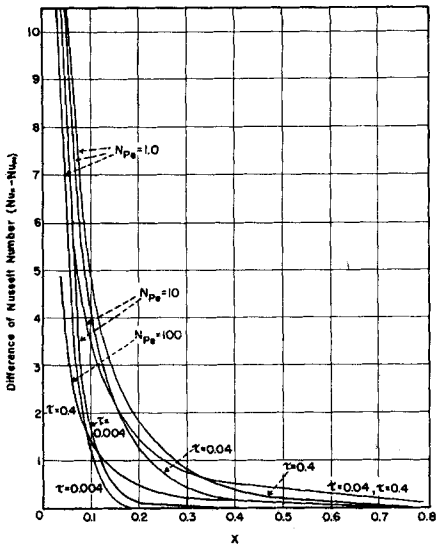

Fig. 8. Nusselt number differences between solutions with and without axial fluid conduction for various times and Peclet numbers.

tion solution. However, the discontinuity in slope exhibited in the solutions neglecting axial conduction, resulting from the joining of a steady state solution to a pure conduction solution, no longer appears. For $\tau > 0.4$, the deviation from the steady state solution is less than 5% for $N_{Pe} = 1$ to 100. Similar results were obtained by Sparrow and Siegel (*14*) in their study of transient laminar flow. At $\tau = 0.4$, the deviations from steady state mean temperature are in the range 0.2 to 2% for $X < 6$ for $N_{Pe} = 1$ and are in the range of 0 to 1% for $X < 6$ for $N_{Pe} = 10$.

The difference between the mean temperatures for case *III* and case *II* during the transient is plotted in Figure 7 for various times and Peclet numbers. It is seen that the axial conduction correction is maximum in the entrance region, which enlarges as time increases. The differences for $N_{Pe} = 10$ are much less than those for $N_{Pe} = 1.0$ for all times and for $N_{Pe} = 100$ are very small (~ 0.001), which cannot be shown in the figure.

On the other hand, the Nusselt number correction is quite significant close to the origin, in view of the leading edge temperature singularity. Also, the difference between the Nusselt numbers for cases II and III, Figure 8, becomes more important as steady state is approached.

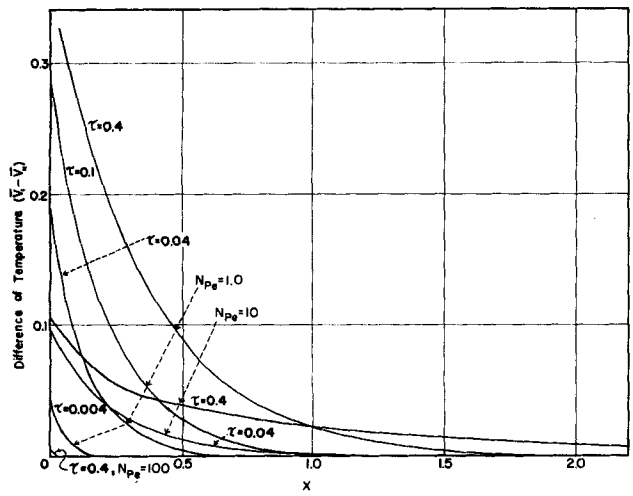

Fig. 9. Mean temperature difference between cases of infinite and semi-infinite parallel plates with axial fluid conduction for various times and Peclet numbers.

Again, the effect is most pronounced at the lower Peclet numbers.

Finally, the difference between the mean temperatures V_I and V_{II} is shown in Figure 9. Axial conduction was taken into account in both cases, but a temperature boundary condition was applied at $X = 0$ in *II* and at $X = -\infty$ in *I*. Again, the correction increases as steady state is approached and for $N_{Pe} \geq 100$ is negligible for all times in the entire downstream region. After steady state is reached, the difference in the mean temperatures is negligible for $X \geq 0.2$ at $N_{Pe} = 1.0$ and for $X \geq 3$ at $N_{Pe} = 10$.

ACKNOWLEDGMENT

This work was supported in part by a grant from the National Science Foundation.

NOTATION

a_1 = see Equation (16)
a_2 = $B/2$
a_3 = see Equation (5)
A = see Equation (3)
A_1 = see Equation (22)
b = radius of tube, or distance between flat plates
$B = N_{Pe}$ = Peclet number, Ub/κ
D = see Equation (16)
n = positive integer
p = Laplace transform variable related to τ
r = radius of tube
R = r/b
t = time
U = uniform fluid velocity
v = temperature
v_o = initial temperature
v_w = wall temperature for $X > 0$
V = dimensionless temperature, $(v - v_o)/(v_w - v_o)$
x = coordinate in direction of flow
X = x/b
y = coordinate perpendicular to flow
Y = y/b

Subscripts

κ = thermal diffusivity
ξ_i = Bessel function eigenvalue
τ = dimensionless time, $(t\kappa)/(b)$

H = Hankel transformed variable
p = Laplace transformed variable
s = sine transformed variable

LITERATURE CITED

1. Chu, S. C., Ph.D. thesis, Northwestern Univ., Evanston, Illinois (1963).
2. Siegel, R., *J. Appl. Mech.*, **26**, 140 (1959).
3. Schneider, P. J., *Trans. Am. Soc. Mech. Engrs.*, **79**, 766 (1957).
4. Bodnarescu, M. V., *VDI-Forsch.*, **216**, 19 (1955).
5. Singh, S. N., *Appl. Sci. Res.*, **A7**, 237 (1958).
6. *Ibid.*, 325.
7. Labuntsov, D. A., *Dokl. Akad. Nauk (SSSR)*, **6**, 1118 (1958).
8. Agrawal, H. C., *Appl. Sci. Res.*, **A9**, 177 (1960).
9. Pahor, S., and J. Strand, *ibid.*, **A10**, 81 (1961).
10. Horvay, G., *J. Heat Transfer*, **83**, 391 (1961).
11. ———, and M. Da Costa, *ibid.*, **86**, 265 (1964).
12. Sneddon, I. N., "Fourier Transforms," McGraw-Hill, New York (1951).
13. Wilson, H. A., *Camb. Phil. Soc. Proc.*, **12**, 406 (1903).
14. Siegel, R., and E. M. Sparrow, *J. Heat Transfer*, **81**, 29 (1959).

Manuscript received August 25, 1964; revision received December 18, 1964; paper accepted December 21, 1964.